Salidroside rescues hypoxic cardiomyocytes by regulating the EGLN1/HIF-1α pathway

WENMAO ZHANG[1], ZILING LIAO[1], CHENGFENG XU[2] and XINPING LIN[1]

[1]Department of Scientific Research, Yueyang Maternal and Child Health-Care Hospital, Yueyang, Hunan 414000, P.R. China; [2]Department of Research and Development, Beijing Zhongwei Research Center of Biological and Translational Medicine, Beijing 100000, P.R. China

Received July 16, 2024; Accepted September 12, 2024

DOI: 10.3892/br.2024.1868

Abstract. Myocardial infarction is characterized by oxygen deficiency caused by arterial flow restriction. Salidroside (SAL) protects against myocardial damage via antioxidant production and inhibition of apoptosis. The present study aimed to investigate potential rescue mechanism of SAL on hypoxic cardiomyocytes. H9C2 cardiomyocytes were divided into normoxia, hypoxia and hypoxia + SAL groups. The inhibitory rate of hypoxia and the optimal concentration and rescue effect of SAL were determined using Cell Counting Kit-8 assay and flow cytometry. Ca^{2+} concentration following hypoxia treatment and SAL intervention were detected by Fluo-4/acetoxymethyl. Tandem mass tag (TMT) proteomics was used to analyze the differential expression of hypoxia-associated proteins among the three groups. SAL exerted a protective effect on hypoxia-injured cardiomyocytes by enhancing aerobic metabolism during hypoxia and rescuing cardiomyocytes from hypoxic damage. SAL promoted cell proliferation, decreased apoptosis and increased Ca^{2+} levels in cell membranes of hypoxic cardiomyocytes. TMT proteomics results showed that the expression levels of intracellular hypoxia inducible factor-1 (HIF)-1α and Egl-9 family HIF 1 (EGLN1) in H9C2 cells were elevated under hypoxic conditions. However, SAL significantly decreased expression levels of HIF-1α and EGLN1. SAL inhibited mitochondrial calcium overload in hypoxic cardiomyocytes and attenuated expression of hypoxia-associated factors. SAL exerted its rescue effect on hypoxic cardiomyocytes through the EGLN1/HIF-1α pathway, thereby suppressing cardiomyocyte apoptosis, improving mitochondrial energy metabolism efficiency and rescuing cardiomyocytes from hypoxic injury.

Correspondence to: Professor Xinping Lin, Department of Scientific Research, Yueyang Maternal and Child Health-Care Hospital, 520 Baling East Road, Yueyang, Hunan 414000, P.R. China
E-mail: linxingping2022@163.com

Key words: myocardial hypoxia, salidroside, Egl-9 family hypoxia inducible factor 1, hypoxia inducible factor-1α, proteomics

Introduction

Myocardial infarction is a condition characterised by inadequate blood supply due to blockage of coronary arteries, leading to increased oxygen demand of tissues because of oxygen deficiency caused by arterial flow restriction (1). Oxygen is an essential factor that affects cell activity and the ultimate electron acceptor in the electron transport chain (ETC), making it key for cell survival. A hypoxic environment damages the ETC, limiting oxygen for mitochondrial consumption to produce ATP via oxidative phosphorylation (2,3). Hypoxia increases pulmonary arterial pressure, resulting in acute pulmonary vasoconstriction (4). Hypoxia is the primary cause of myocardial cell injury. It inhibits proliferation of myocardial cells, induces apoptosis and decreases the viability of myocardial cells (5-7).

Rhodiola rosea L., a perennial herb with various biological effects, was first used in Tibetan medicine to treat hypoxia, decrease altitude illness, lower blood pressure and improve oxygen utilisation and tolerance to hypoxia (8-10). *R. rosea L.* improves aerobic metabolic processes during hypoxia and exerts a protective effect on cardiomyocytes damaged by hypoxia. Salidroside (SAL), a phenolic glycoside compound isolated from *R. rosea L.*, exhibits various pharmacological properties, including antioxidative, anti-apoptotic, anti-inflammatory and cardioprotective effects (6,11). SAL plays an important role in protecting against myocardial damage and has significant inhibitory and protective effects on damaged myocardial tissue via antioxidant production and inhibition of myocardial apoptosis (12,13). In cardiovascular disease, SAL has been reported to enhance and protect cardiac function by inhibiting cardiomyocyte degeneration, necrosis and apoptosis (14). SAL can also stimulate the accumulation of hypoxia inducible factor (HIF)-1α under hypoxia conditions, decrease hypoxia-induced injury of cells and protect cardiomyocytes from hypoxia/reoxygenation injury, indicating the potential of SAL in combating hypoxia injury (6,15,16). Furthermore, SAL alleviates cardiovascular emergency contraction caused by hypoxia, induces and improves activity of key enzymes for free radical scavenging in the body, promotes balance between free radical generation and scavenging and inhibits lipid peroxidation in the cell membrane (17-19). SAL can help resist hypoxic injury, participate in signalling pathways that

antagonise hypoxic cytotoxicity and resist hypoxia-induced apoptosis by reducing the expression of associated proteins such as PI3K and AMPK, which effectively protects against ischaemic anoxic cardiovascular disease (12,13,20,21).

HIF-1 is an oxygen-regulated transcription activator that is activated because of the growth restriction of cells in hypoxia owing to blockage of oxidative phosphorylation in normal cells, consequently making glycolysis the primary energy supply mode (22). HIF-1 consists of α- and β-subunits, which are key gene regulators involved in cellular hypoxia response, erythropoiesis regulation, angiogenesis, anaerobic metabolism and glycolysis pathways (23,24). HIF-1α is a key factor that influences hypoxic response in tumour cells and is expressed cumulatively under hypoxia conditions; however, its expression levels are low under normoxic conditions (24). In addition, HIF-1α regulates cell response to hypoxia and tumour biological behaviour by influencing cell apoptosis/proliferation and energy metabolism (25).

Egl-9 family HIF 1 (EGLN1) is the primary oxygen receptor in the human body (26). Under normoxic conditions, EGLN1 uses O_2 as a cofactor to hydroxylate HIF-1α. HIF-1α is recognised by the E3 ubiquitin ligase complex formed by the von Hippel-Lindau protein, resulting in its rapid degradation by proteasomes (27). However, under hypoxic conditions, activity of the proline hydroxylase EGLN1 is inhibited, which inhibits the hydroxylation and ubiquitination-based degradation of HIF-1α. This causes HIF-1α to accumulate and enter the nucleus to form a complex with HIF-1β (28). This complex regulates expression of genes downstream of hypoxia and hypoxic stress response in the body (29).

Since hypoxia-induced apoptosis of cardiomyocytes is a notable risk factor for cardiovascular disease (30,31), preventing cardiomyocyte apoptosis under hypoxic conditions is key. SAL alleviates cardiomyocyte apoptosis and enhances cell viability; however, the underlying mechanisms remain unclear. Studies on SAL have mainly focused on its ability to resist hypoxia and the mechanism underlying its anti-hypoxic effects (6,12,13); however, whether SAL mitigates existing hypoxic conditions remains to be determined. Furthermore, whether there is a regulatory interaction between EGLN1 and HIF-1α that affects apoptosis of cardiomyocytes is unknown. Therefore, the rescue ability of SAL in hypoxic H9C2 cells was studied using hypoxic culture conditions in.

Materials and methods

Materials. SAL, DMSO, trypsin, 1.5 M Tris-HCl (pH=8.8), 1.0 M Tris-HCl (pH=6.8) and penicillin-streptomycin solution were purchased from Beijing Solarbio Science & Technology Co., Ltd. Serum-free DMEM and FBS were purchased from Thermo Fisher Scientific, Inc. PBS was purchased from Lanzhou Bailing Biotech Co., Ltd. RNApure Tissue & Cell (DNase I), UltraSYBR One Step RT-qPCR, HiFiScript cDNA Synthesis and Cell Counting Kit-8 (CCK-8) were purchased from Beijing ComWin Biotech Co., Ltd. SDS-PAGE Sample Loading Buffer (5X), fluo-4/acetoxymethyl ester (Fluo-4/AM) (2 mM) and Annexin V-FITC Apoptosis Detection kit were purchased from Beyotime Institute of Biotechnology. BCA protein assay kit and 5% bovine serum albumin (BSA) were purchased from Beijing Labgic Co., Ltd. L-glutamine was purchased from Suzhou Haixing Biological Technology Co., Ltd.; 30% acrylamide (29:1) was purchased from Sinopharm Chemical Reagent Co., Ltd. PVDF membranes was purchased from MilliporeSigma. Tween-20 was purchased from Amresco Co., Ltd. Anti-EGLN1 (cat. no. #4835s) was purchased from Cell Signaling Technology, Inc. Anti-HIF-1α (cat. no. NB100-105) was purchased from Novus Biologicals, LLC. Anti-GAPDH (cat. no. 60004-1-Ig) was purchased from Proteintech Group, Inc. Horseradish peroxidase-conjugated AffiniPure Goat Anti-Rabbit IgG (cat. no. ZB2301) was purchased from OriGene Technologies, Inc. 10% SDS was purchased from China Sinopharm International (Shanghai) Co., Ltd. Enhanced chemiluminescence (cat. no. ECL-0011) was purchased from Ding Guo Prosperous Co., Ltd. Primers for HIF-1α (forward, 5'-CCGCCACCACCACTGATGAATC-3' and reverse, 5'-GTGAGTACCACTGTATGCvTGATGCC-3') and GAPDH (forward, 5'-GAAGGTCGGTGTGAACGGAT-3' and reverse, 5'-CCCATTTGATGTTAGCGGGAT-3') were purchased from Beijing Tsingke Biotech Co., Ltd. EGLN1 primers (forward, 5'-AGCTGGTCAGCCAGAAGAGT-3' and reverse, 5'-GCC CTCGATCCAGGTGATCT-3') were purchased from Sangon Biotech Co., Ltd. All other solvents and chemicals were of analytical grade. Pure water was produced using a Milli-Q purification system (MilliporeSigma).

Cell culture. H9C2 cell line was purchased from Suzhou Haixing Biological Technology Co., Ltd. The cells in the normoxia group were cultured in DMEM containing 10 FBS and 1% penicillin-streptomycin and incubated at 37˚C in a 5% CO_2 incubator. For the hypoxia group, cells were cultured at 37˚C with 5 CO_2 and 2% O_2.

In vitro cell CCK-8 assay. The biocompatibility of SAL in H9C2 cells was assessed using CCK-8 assay. H9C2 cells were seeded into 96-well plates at a density of $1x10^5$ cells/well and incubated overnight at 37˚C, following which 200 μl SAL (10, 100, 250, 500, 750 and 1,000 nM) or DMEM (blank control) was added for an additional 24 h at 37 ˚C. After removing the DMEM, 110 μl fresh medium (containing 10 μl CCK-8) was added and incubated for 1.5 h. Finally, viability was determined by measuring the absorbance of each well at 450 nm using Spectrophotometer Multiskan (Thermo Fisher Scientific, Inc.).

The ability of SAL to rescue hypoxia-treated H9C2 cells was also confirmed using the CCK-8 method. H9C2 cells were cultured in 96-well plates at a density of $1x10^5$ cells/well and incubated overnight at 37˚C. H9C2 cells were transferred to a hypoxic incubator and cultured under hypoxic conditions for 48 h at 37˚C. Medium was removed and 200 μl SAL (10, 100, 250, 500, 750 and 1,000 nM) or an equal volume of fresh DMEM was added for 24 h in the hypoxic incubator at 37˚C. After removing DMEM, the cells were incubated with CCK-8 solution for 1.5 h. Finally, viability was calculated by measuring the absorbance of each well at 450 nm using Spectrophotometer Multiskan (Thermo Fisher Scientific, Inc.).

Early and late apoptosis analysis. The rescue effect of SAL on hypoxic cells was quantitatively analysed using flow cytometry. H9C2 cells were co-inoculated into 3-cm dishes at a density of $2.5x10^5$ cells/ml. A total of three groups was used: Normoxia, hypoxia and hypoxia + SAL. Cells in the normoxia group were cultured under normoxic conditions for 48 h and

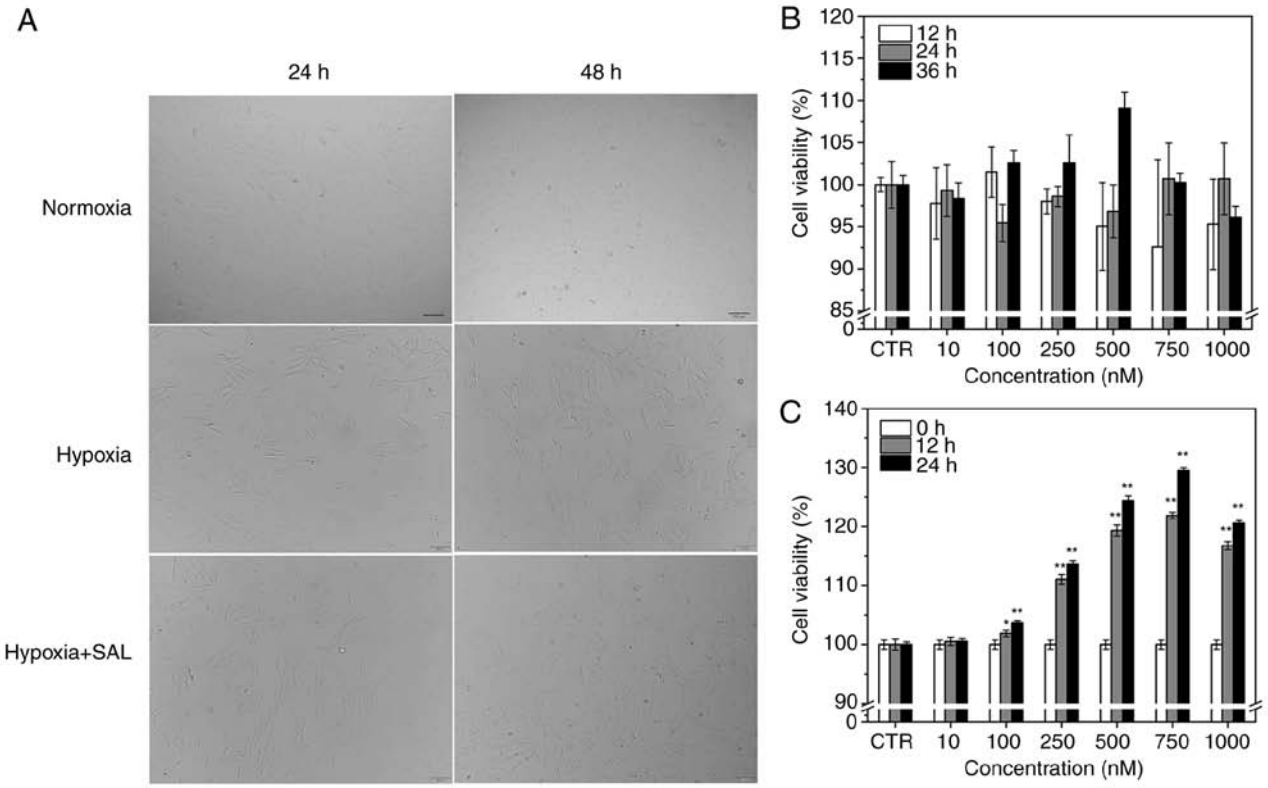

Figure 1. SAL increase the survival rates of H9C2 cells under hypoxic condition. (A) Cell morphology changes (scale bar, 100 μm). Viability of H9C2 cells following incubation with different concentrations of SAL for different time under (B) normoxic or (C) hypoxic conditions. *P<0.05, **P<0.01 vs. CTR. SAL, Salidroside; CTR, Control.

incubated in fresh DMEM for an additional 24 h at 37˚C. Cells in the hypoxia group were incubated under hypoxic conditions for 48 h at 37˚C, followed by incubation in DMEM for an additional 24 h. In the hypoxia + SAL group, cells were incubated under hypoxic conditions for 48 h at 37˚C, followed by incubation with 200 μl SAL (100 nM) for an additional 24 h at 37˚C. Cells were collected via centrifugation (500 x g for 5 min at 4˚C) and washed twice with PBS. Cells were suspended in 100 μl binding buffer mixed with 5 μl Annexin-V/FITC and incubated for 5 min in the dark at room temperature. The cells were mixed with 10 PI stain and 400 μl PBS. The stained cells were analyzed by flow cytometry (BD Biosciences) and analysed using WinCyte software (CompuCyte).

Intercellular Ca^{2+} concentration analysis. The ability of SAL to maintain intracellular calcium homeostasis was evaluated using Fluo-4/AM. H9C2 cells were cultured in 12-well plates with cell slides at a density of $1.5x10^5$ cells/well. Normoxia group was cultured at 37˚C with 5% CO_2 and 2% O_2. Hypoxia group was cultured at 37˚C with 5% CO_2. The culture medium was removed following incubation, the cells were washed with PBS twice and 200 μl Fluo-4/AM (2.5 μM) was added. The cells were then incubated at 37˚C for 15 min in the dark. The stained H9C2 cells were washed with PBS three times, 300 μl 4% paraformaldehyde was added to fix the cells for 30 min at 37˚C, and cells were observed under a fluorescence microscope at 100x magnification (Leica GmbH).

Tandem mass tag (TMT) proteomics analysis. A total of $1x10^7$ cells/tube (three tubes from each group) were subjected to TMT proteomic analysis to screen differentially expressed proteins, which were analysed at the functional level as reported (32). Gene Ontology (GO; david.ncifcrf.gov/tools.jsp) and Kyoto Encyclopaedia of Genes and Genomes (KEGG) enrichment (http://www.kegg.jp) analyses were performed to determine whether differentially expressed proteins were significantly enriched in hypoxia-related pathways. For each protein, the fold-change (FC) was calculated as the ratio of mean values of all biological measurements in each two groups.

Reverse transcription-quantitative (RT-q)PCR. RNA was extracted from cells using an RNApure Tissue and Cell kit (DNase I) according to the manufacturer's protocol. cDNA was synthesised using HiFiScript cDNA Synthesis kit according to the manufacturer's protocol. UltraSYBR One Step RT-qPCR Kit was used to detect the expression of HIF-1α and EGLN1. Thermocycling conditions were as follows: Initial denaturation at 95˚C for 30 sec, followed by 45 cycles of 95˚C for 5 sec and 60˚C for 30 sec. The relative expression levels of HIF-1α and EGLN1 were evaluated by the $2^{-\Delta\Delta Cq}$ method (33).

Western blotting. Cell lysate was extracted using RIPA assay buffer and protein lysates were obtained following centrifugation (12,000 x g for 10 min at 4˚C). Proteins were quantified using a BCA assay kit. The protein extracts were isolated and transferred onto a PVDF membrane, which was blocked with 5% BSA at 37˚C for 2 h. Subsequently, the membrane was incubated overnight with primary antibody at 4˚C, followed by incubation with secondary antibody at

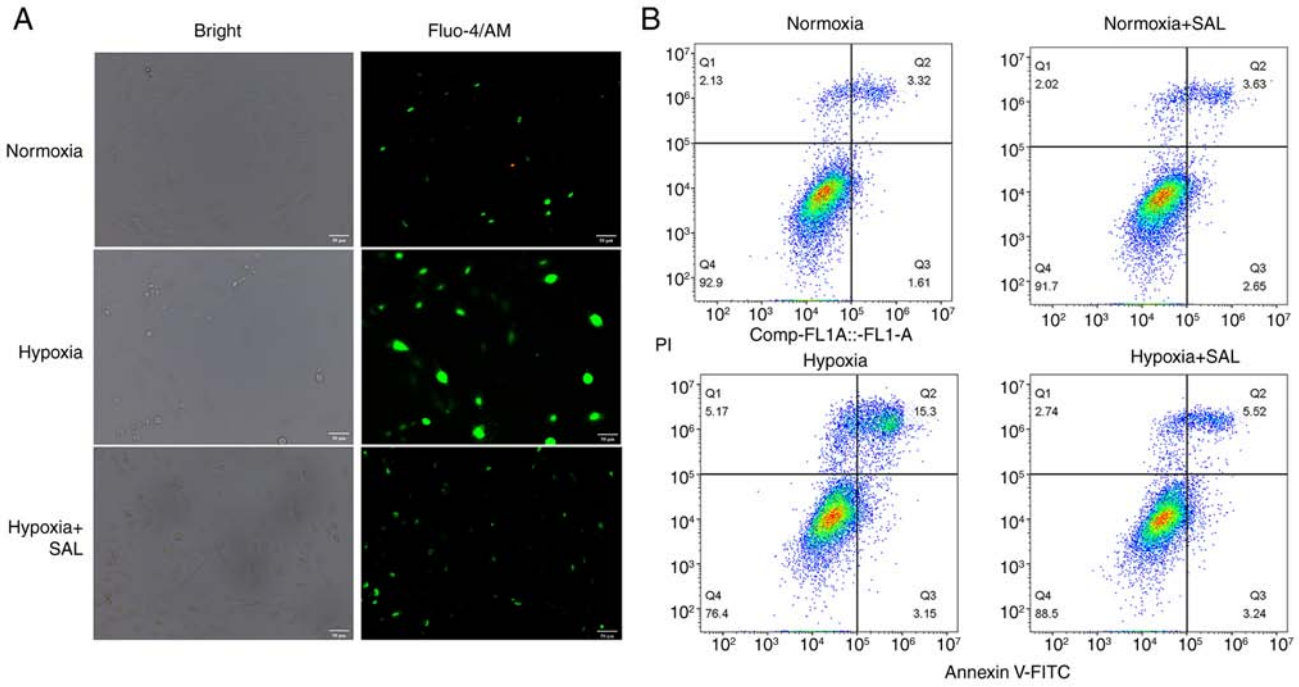

Figure 2. SAL relieved Ca^{2+} overload and reduced apoptosis of H9C2 cell. (A) Fluorescence microscope images of Ca^{2+} detection. (B) Flow cytometry analysis of H9C2 cells. SAL, Salidroside; Fluo-4/AM, fluo-4/acetoxymethyl ester.

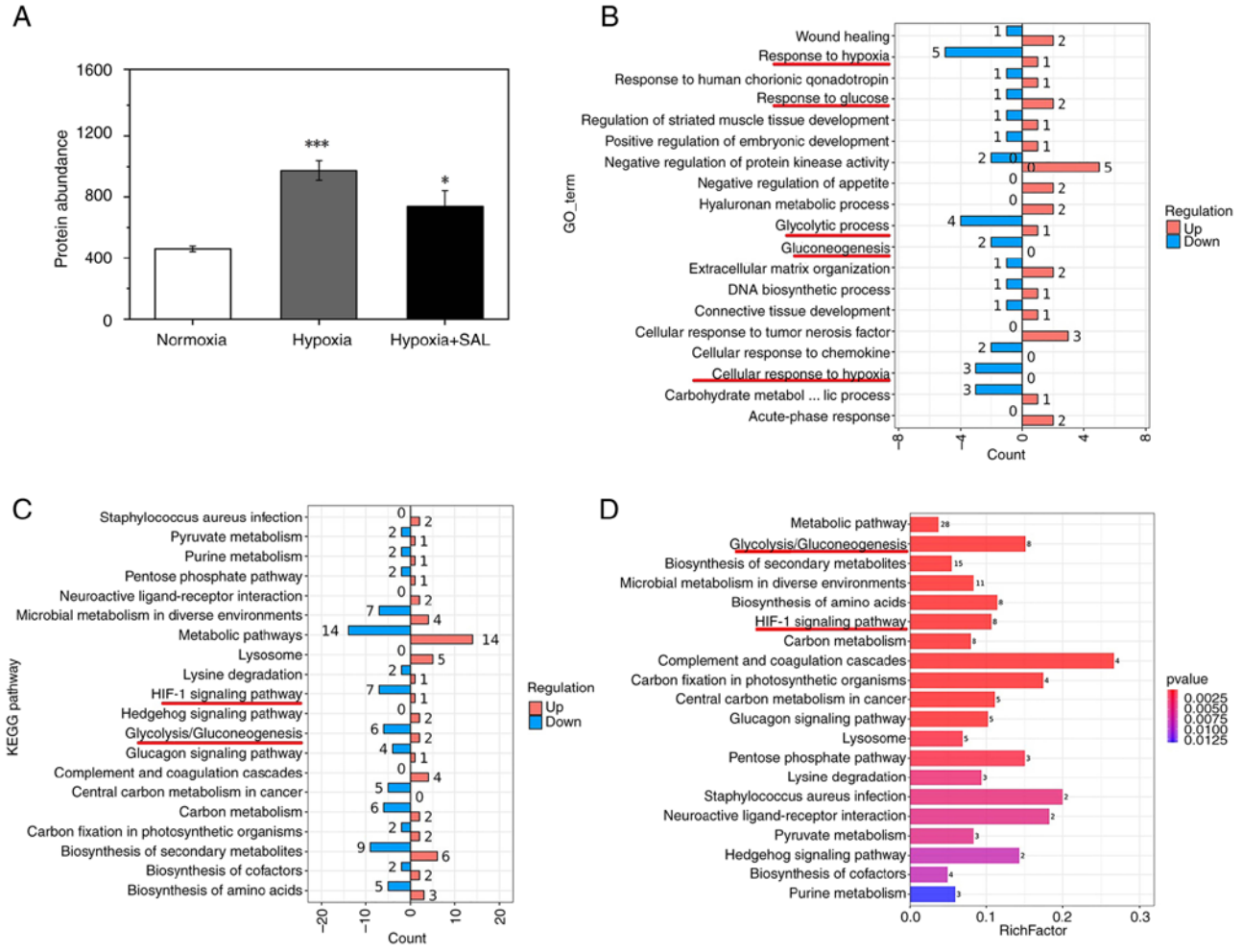

Figure 3. GO enrichment analysis and KEGG enrichment analysis. (A) Protein abundance of Egl-9 family hypoxia-inducible factor 1. (B) Enrichment in biological processes. (C) KEGG enrichment analysis and (D) pathway enrichment. $^{*}P<0.05$, $^{***}P<0.001$ vs. normoxia. SAL, Salidroside; KEGG, Kyoto Encyclopaedia of Genes and Genomes; GO, Gene Ontology. Red lines indicated the term or pathway is glucose metabolism- or hypoxia-related.

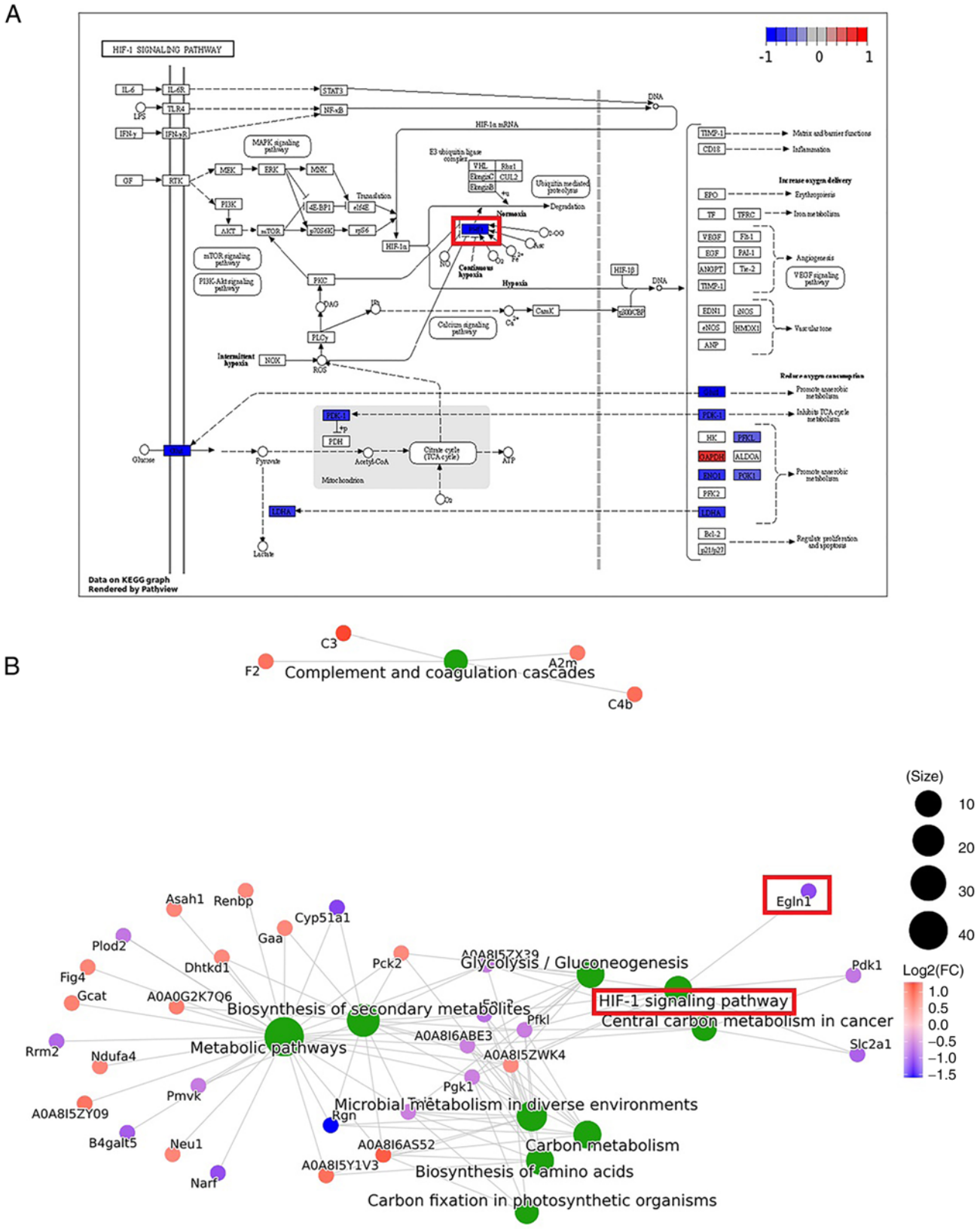

Figure 4. Change in expression of EGLN1 and HIF-1α pathway. EGLN1 in (A) pathway enrichment pathway and (B) pathway enrichment and differential protein network. EGLN1, Egl-9 family hypoxia-inducible factor.

37˚C for 1 h. Chemiluminescent imaging system (Clinx Science) was used to detect the signals. The bands were quantified using Image J software 6.3 (imagej.net/software/).

Statistical analysis. All data were analysed by SPSS 16.0 software (SPSS, Inc.). Continuous variables are expressed as the mean ± standard deviation of three independent replicate experiments. One-way analysis of variance followed by Tukey

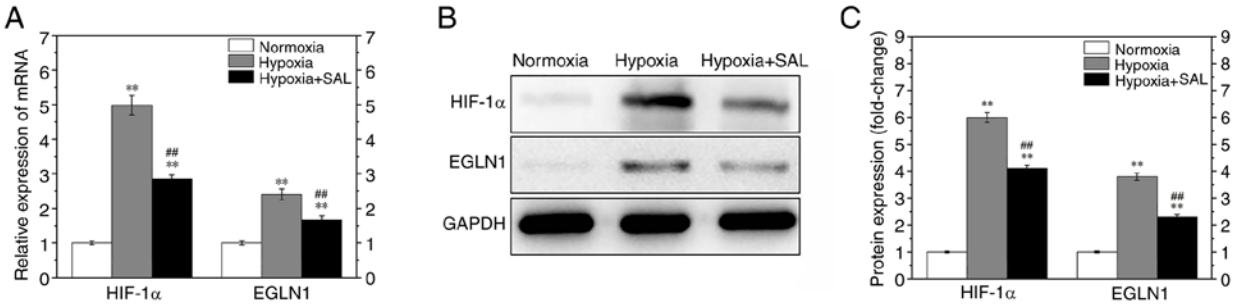

Figure 5. Expression of EGLN1 and HIF-1α. (A) mRNA expression of HIF-1α and EGLN1. (B) SAL reduced the expression of (C) HIF-1α and EGLN1 under hypoxic conditions. **P<0.01 vs. normoxia; $^{\#\#}$P<0.01 vs. hypoxia. HIF, hypoxia-inducing factor; EGLN1, Egl-9 family hypoxia-inducible factor; SAL, Salidroside.

multiple comparisons test were employed to determine significance between different groups. Fisher's exact test was used to find enriched GO and KEGG terms. The corresponding P-value was calculated as the significance index. Benjamini-Hochberg False Discovery Rate was used to correct the P-value. P<0.05 was considered to indicate a statistically significant difference.

Results

Hypoxia modelling and optimal concentration screening of SAL. Hypoxic incubator models create a hypoxic environment and induce cell apoptosis (34,35). Morphology of the adherent H9C2 cells was fusiform; however, following hypoxic culture, the cell morphology became round and some cells fell off the bottom of the culture dish (Fig. 1A). These morphological changes were not apparent in SAL treatment group. Compared with the hypoxia group, cells of the hypoxia + SAL group adhered to culture dishes and exhibited spindle-shaped shape, which was notably improved.

CCK-8 assay was used to evaluate the effect of SAL on viability of H9C2 cells under a normoxic environment (Fig. 1B). Cell viability was >90%, which confirmed good biocompatibility of SAL. The different incubation times had no significant effect on proliferation of H9C2 cells under normoxic conditions; therefore, 24 h was selected as the incubation time for SAL in subsequent experiments.

A hypoxia model was created to explore the ability of SAL to rescue H9C2 cells following hypoxia. With higher SAL concentrations, the survival rates of hypoxic cells were significantly higher than those of the control group (Fig. 1C). SAL concentrations of 100, 250, 500, 750 and 1,000 nM showed good rescue ability; therefore, 100 nM was selected for subsequent experiments.

Ca^{2+} detection and apoptosis. To investigate changes of intracellular Ca^{2+} in the three groups, the cells were stained with Fluo-4/AM and observed using a fluorescence microscope. Compared with the control group, H9C2 cells in the hypoxia group showed brighter green fluorescence, indicating that the hypoxia induced intracellular calcium overload (Fig. 2A). Following SAL treatment in hypoxic cells, green fluorescence intensity of Ca^{2+} was notably weakened compared with the hypoxia group. These results indicated that SAL treatment reduced intracellular calcium overload in hypoxic cells, thereby inhibiting cell apoptosis.

Flow cytometric analysis of cells stained with Annexin V-FITC/PI was used to assess the degree of apoptosis. Survival rates of H9C2 cells in the normoxia and normoxia + SAL groups were >90%, which was consistent with the cell viability results obtained by CCK-8 assay (Fig. 2B). These results further confirmed that SAL has good biocompatibility. After H9C2 cells were cultured under hypoxic conditions, ~18.45% cells were apoptotic and the apoptosis rate increased by 13.5% compared with the normoxia group, indicating that apoptosis was induced via hypoxia-related pathways following hypoxia. In hypoxic cells treated with SAL, the apoptosis rate was 8.76% (early and late apoptosis, 3.24 and 5.52%, respectively), which was 9.69% lower than that in the hypoxia group. Flow cytometry showed that SAL effectively improved survival rate of hypoxic cells and attenuated the effects of hypoxia.

Differential protein screening. According to proteomic analysis, 63 proteins were up- and 42 were downregulated in the normoxia group compared with the hypoxia group. The expression of 78 proteins was up-while that of 48 proteins was downregulated in the normoxia group compared with the hypoxia + SAL group. The expression of four proteins was up- and that of 12 was downregulated in the hypoxia group compared with the hypoxia + SAL group (Fig. S1). Subsequently, differentially expressed proteins were screened for those associated with the hypoxia pathway.

Relative protein abundance of EGLN1 (974) in the hypoxia group was significantly higher than that in the control group (461) following hypoxia treatment; however, the protein abundance decreased to 737 following treatment with SAL (P<0.05; Fig. 3A). EGLN1 expression was negatively associated with oxygen concentration under hypoxic conditions.

GO and KEGG enrichment analysis. GO enriched terms were 'response to glucose', 'response to hypoxia' 'glycolysis/gluconeogenesis' (Fig. 3B). Therefore, cells responded to hypoxia by expressing hypoxia-related proteins; hypoxia treatment affected cellular glucose metabolism pathways. KEGG enrichment analysis showed that HIF-1 signalling pathway was enriched in the hypoxia vs. hypoxia + SAL group; seven proteins were down- and one was upregulated (Fig. 4A and B). Hypoxia affected the glycolysis/gluconeogenesis pathway, a central pathway in energy metabolism (Fig. 3C and D).

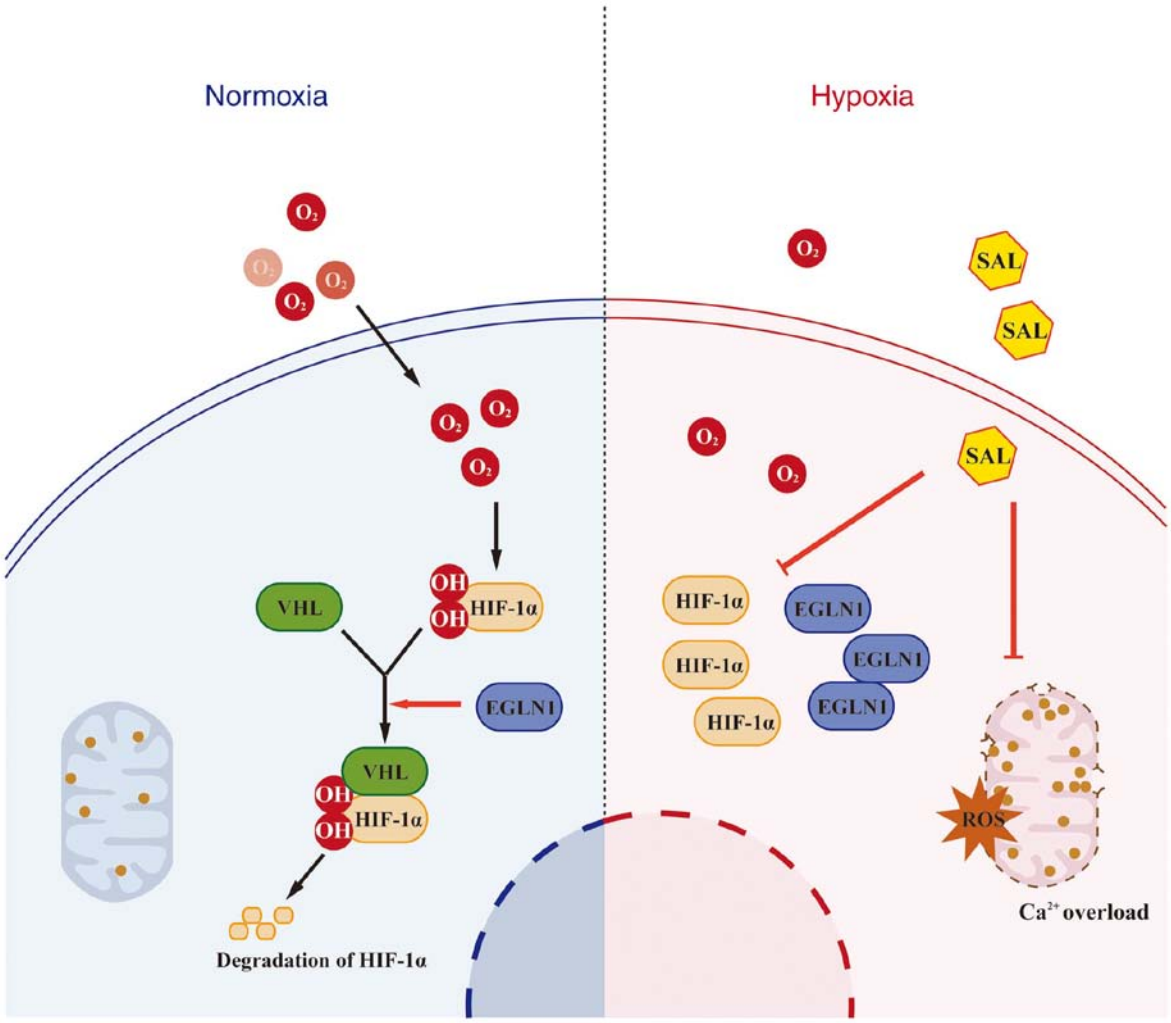

Figure 6. SAL rescues cardiomyocytes under hypoxia. SAL exert its rescue effect on hypoxic cardiomyocytes through the EGLN1/HIF-1α pathway; SAL suppress cardiomyocyte apoptosis, improve mitochondrial energy metabolism efficiency, and rescue cardiomyocytes from hypoxic injury. SAL, Salidroside; VHL, von Hippel-Lindau; HIF, hypoxia-inducing factor; EGLN, Egl-9 family hypoxia-inducible factor; ROS, reactive oxygen species.

Expression of HIF-1α and EGLN1. Expression of HIF-1α and EGLN1 in the hypoxia group was significantly higher than those in the normoxia group (Fig. 5A). For HIF-1α, mRNA expression under hypoxia was 4.98-fold that of the control group, whereas treatment with SAL decreased its expression. The mRNA expression levels of EGLN1 showed a similar trend. mRNA expression of EGLN1 under hypoxia was 2.40-fold higher than that in the normoxia group and the expression of EGLN1 was reduced following co-incubation with SAL. Non-hydroxylated HIF-1α is more stable than hydroxylated HIF-1α, resulting in increased mRNA expression. EGLN1 mRNA expression increased under hypoxia.

Compared to the normoxia group, expression of HIF-1α protein significantly increased following hypoxia treatment, which was consistent with mRNA levels (Fig. 5B and C). EGLN1 protein expression increased following hypoxia treatment. However, following treatment with SAL for 24 h, expression of HIF-1α and EGLN1 protein decreased.

Discussion

Under hypoxic conditions, the ETC in the mitochondria of cardiomyocytes is blocked due to insufficient oxygen supply (36). Electrons leak out of the respiratory chain and combine with O_2 to produce reactive oxygen species (ROS), causing lipid peroxidation of mitochondrial and cell membranes and ultimately apoptosis (36,37). Therefore, it is key to prevent hypoxia-induced loss of cardiomyocytes. Studies have shown that SAL exerts anti-hypoxic and protective effects on cardiac function (12,13,38). Following hypoxic stimulation *in vitro*, SAL treatment improves cardiomyocyte activity, protects cardiomyocytes from hypoxia-induced injury and decreases apoptosis (39). The present study further demonstrated that SAL could rescue cardiomyocytes under hypoxia, decrease apoptosis and regulate the hypoxia-associated EGLN1/HIF-1α pathway.

Cobalt chloride ($CoCl_2$) is used to mimic hypoxic conditions because it promotes apoptosis and increases ROS production, leading to mitochondrial abnormality (40). However, $CoCl_2$ mimics hypoxia by stabilising HIF-1α expression (41). Therefore, the present study used true hypoxia (2% O_2). The present study showed that SAL could effectively relieve Ca^{2+} overload in hypoxic cells. Hypoxia changes cell membrane potential, leading Ca^{2+} to enter the cells, thereby causing calcium overload. Calcium ions play an important role in several physiological processes, such as energy production and apoptosis (42,43).

Mitochondrial calcium overload induces mitochondrial swelling, mitochondrial membrane potential disorder and the release of apoptotic factors into cytoplasm, which in turn leads to apoptosis (44,45). In cardiomyocytes, mitochondria contain large calcium pools; when mitochondrial Ca^{2+} levels exceed their capacity, mitochondrial permeability transition pores are irreversibly opened, lowering mitochondrial membrane potential and ultimately causing apoptosis. Decreasing mitochondrial Ca^{2+} overload can therefore prevent cardiac injury (46). Here, SAL decreased Ca^{2+} concentration in cardio myocytes under hypoxic condition, which may also play a protective role.

TMT proteomics identified differentially expressed proteins associated with glucose metabolism and the hypoxia response pathway, among which EGLN1 plays an important role in hypoxia (26,27). Hypoxia inhibits activation of EGLN1, which in turn inhibits hydroxylation of the two proline residues of HIF-1α, causing HIF-1α to accumulate in the cell and promoting apoptosis. The addition of SAL alleviates effects of hypoxia environment, EGLN1 protein is activated and hydroxylates the oxygen-dependent degradation domain of HIF-1α, causing its degradation (27). SAL treatment downregulated HIF-1α and EGLN1 expression, which was increased under hypoxia. GO and KEGG analysis showed that EGLN1 protein expression was related to HIF-1α hypoxia pathway. As the upstream gene of HIF-1α, EGLN1 expression and activity directly affect the expression of HIF-1α, thus affecting apoptosis. However, SAL decreased expression of HIF-1α and EGLN1 and increased the vitality of cells.

This HIF-1α pathway is key for cellular adaptation and survival in hypoxic environments. When cells are exposed to hypoxia, HIF-1α is stabilised and dimerises with HIF-1β, which regulates the expression of genes involved in metabolism, cell proliferation and apoptosis. Several other differentially expressed proteins involved in the HIF-1 signalling pathway have been identified by TMT proteomics, including downstream metabolic regulators of HIF-1α, such as pyruvate dehydrogenase kinase (PDK1) and lactate dehydrogenase (LDHA) (47). Under hypoxic conditions, HIF-1-mediated PDK1 expression shunts glucose away from mitochondria, attenuating mitochondrial respiration and preventing toxic ROS production (48). LDHA is a key enzyme that converts pyruvate into lactic acid during glycolysis. Hypoxia-induced LDHA is reported to promote inflammation (47,49). SAL alleviates hypoxia-induced upregulation of PDK1 and LDHA, suggesting that SAL may alleviate physiological stress caused by hypoxia (47,49). The expression of HIF-1α and EGLN1 increased under hypoxia treatment; the expression of HIF-1α decreased following treatment with SAL, demonstrating that SAL decreased expression of hypoxia factors. Similarly, EGLN1 showed a consistent trend with HIF-1α. These results showed that SAL inhibited expression of hypoxia-related factors, inhibiting their effects in the signalling pathway and achieving cell rescue. SAL could effectively regulate the expression of HIF-1α and EGLN1 by regulating the EGLN1/HIF-1α hypoxia signalling pathway and inhibit apoptosis.

The GO and KEGG enrichment analysis also showed hypoxia affected the glycolysis/gluconeogenesis pathway, a central pathway in energy metabolism Gluconeogenesis refers to the process by which non-sugar substances are converted into glycogen or glucose by enzymes in organs such as the liver and kidney (50,51). HIF-1 activation by hypoxia induces glycolysis, the anaerobic oxidation of glucose, resulting in conversion of normoxic aerobic respiratory metabolic pathway to a different energy production pathway with lower oxygen consumption (50).

The rescue effect and underlying mechanism of action of SAL on cardiomyocytes remain to be confirmed in cell lines other than H9C2 cells. The concentrations required to achieve potential effects of SAL may vary in different cells; therefore, further investigation is warranted to optimize the concentration of SAL for hypoxia treatment.

In conclusion, SAL enhanced the viability of cardiomyocytes, inhibited intracellular mitochondrial calcium overload, decreased the expression of hypoxia-associated factors HIF-1α and EGLN1 and inhibited cell apoptosis through the EGLN1/HIF-1α pathway, suggesting that SAL effectively rescued the damage of cardiomyocytes caused by hypoxia (Fig. 6).

Acknowledgements

Not applicable.

Funding

The present study was supported by the Natural Science Foundation of Hunan Province (grant no. 2023JJ50289) and Scientific Research Project of Hunan Provincial Health Commission (grant no. 202103011065).

Availability of data and materials

The data generated in the present study may be requested from the corresponding author.

Authors' contributions

WZ wrote and reviewed the manuscript and conceived and designed the study. ZL performed experiments and analyzed data. CX performed experiments. XL conceived and designed the study and edited the manuscript. WZ and XL confirm the authenticity of all the raw data. All authors have read and approved the final manuscript.

Ethics approval and consent to participate

Not applicable.

Patient consent for publication

Not applicable.

Competing interests

The authors declare that they have no competing interests.

References

1. Veldhuizen J, Chavan R, Moghadas B, Park JG, Kodibagkar VD, Migrino RQ and Nikkhah M: Cardiac ischemia on-a-chip to investigate cellular and molecular response of myocardial tissue under hypoxia. Biomaterials 281: 121336, 2022.

2. Ichiki T and Sunagawa K: Novel roles of hypoxia response system in glucose metabolism and obesity. Trends Cardiovasc Med 24: 197-201, 2014.
3. Kishimoto I, Tokudome T, Hosoda H, Miyazato M and Kangawa K: Ghrelin and cardiovascular diseases. J Cardiol 59: 8-13, 2012.
4. Wilkins MR, Ghofrani HA, Weissmann N, Aldashev A and Zhao L: Pathophysiology and treatment of high-altitude pulmonary vascular disease. Circulation 131: 582-590, 2015.
5. Guo J, Zhu K, Li Z and Xiao C: Adiponectin protects hypoxia/reoxygenation-induced cardiomyocyte injury by suppressing autophagy. J Immunol Res 2022: 8433464, 2022.
6. Liu B, Wei H, Lan M, Jia N, Liu J and Zhang M: MicroRNA-21 mediates the protective effects of salidroside against hypoxia/reoxygenation-induced myocardial oxidative stress and inflammatory response. Exp Ther Med 19: 1655-1664, 2020.
7. Rabinovich-Nikitin I, Blant A, Dhingra R, Kirshenbaum LA and Czubryt MP: NF-κB p65 attenuates cardiomyocyte PGC-1α expression in hypoxia. Cells 11: 2193, 2022.
8. Chen Y, Tang M, Yuan S, Fu S, Li Y, Li Y, Wang Q, Cao Y, Liu L and Zhang Q: *Rhodiola rosea*: A therapeutic candidate on cardiovascular diseases. Oxid Med Cell Longev 2022: 1348795, 2022.
9. Li Y, Zhao Y, Li X, Liu T, Jiang X and Han F: Characterization of global metabolic profile of Rhodiola crenulata after oral administration in rat plasma, urine, bile and feces based on UHPLC-FT-ICR MS. J Pharm Biomed Anal 149: 318-328, 2018.
10. Xie N, Fan F, Jiang S, Hou Y, Zhang Y, Cairang N, Wang X and Meng X: Rhodiola crenulate alleviates hypobaric hypoxia-induced brain injury via adjusting NF-κB/NLRP3-mediated inflammation. Phytomedicine 103: 154240, 2022.
11. Bai XL, Deng XL, Wu GJ, Li WJ and Jin S: Rhodiola and salidroside in the treatment of metabolic disorders. Mini Rev Med Chem 19: 1611-1626, 2019.
12. Chen L, Liu P, Feng X and Ma C: Salidroside suppressing LPS-induced myocardial injury by inhibiting ROS-mediated PI3K/Akt/mTOR pathway in vitro and in vivo. J Cell Mol Med 21: 3178-3189, 2017.
13. Tian X, Huang Y, Zhang X, Fang R, Feng Y, Zhang W, Li L and Li T: Salidroside attenuates myocardial ischemia/reperfusion injury via AMPK-induced suppression of endoplasmic reticulum stress and mitochondrial fission. Toxicol Appl Pharmacol 448: 116093, 2022.
14. Yan W, Li K, Buhe A, Li T, Tian P and Hong J: Salidroside inhibits the proliferation and migration of gastric carcinoma cells and tumor growth via the activation of ERS-dependent autophagy and apoptosis. RSC Adv 9: 25655-25666, 2019.
15. Chen X, Kou Y, Lu Y and Pu Y: Salidroside ameliorated hypoxia-induced tumorigenesis of BxPC-3 cells via down-regulating hypoxia-inducible factor (HIF)-1α and LOXL2. J Cell Biochem 121: 165-173, 2020.
16. Tang Y, Hou Y, Zeng Y, Hu Y, Zhang Y, Wang X and Meng X: Salidroside attenuates $CoCl_2$-simulated hypoxia injury in PC12 cells partly by mitochondrial protection. Eur J Pharmacol 912: 174617, 2021.
17. Hou Y, Zhang Y, Jiang S, Xie N, Zhang Y, Meng X and Wang X: Salidroside intensifies mitochondrial function of $CoCl_2$-damaged HT22 cells by stimulating PI3K-AKT-MAPK signaling pathway. Phytomedicine 109: 154568, 2023.
18. Wang YF, Chang YY, Zhang XM, Gao MT, Zhang QL, Li X, Zhang L and Yao WF: Salidroside protects against osteoporosis in ovariectomized rats by inhibiting oxidative stress and promoting osteogenesis via Nrf2 activation. Phytomedicine 99: 154020, 2022.
19. Xing Y, Peng HY, Li X, Zhang MX, Gao LL and Yang XE: Extraction and isolation of the salidroside-type metabolite from zinc (Zn) and cadmium (Cd) hyperaccumulator Sedum alfredii Hance. J Zhejiang Univ Sci B 13: 839-845, 2012.
20. Xu MC, Shi HM, Gao XF and Wang H: Salidroside attenuates myocardial ischemia-reperfusion injury via PI3K/Akt signaling pathway. J Asian Nat Prod Res 15: 244-252, 2013.
21. Zhu Y, Shi YP, Wu D, Ji YJ, Wang X, Chen HL, Wu SS, Huang DJ and Jiang W: Salidroside protects against hydrogen peroxide-induced injury in cardiac H9c2 cells via PI3K-Akt dependent pathway. DNA Cell Biol 30: 809-819, 2011.
22. Godet I, Shin YJ, Ju JA, Ye IC, Wang G and Gilkes DM: Fate-mapping post-hypoxic tumor cells reveals a ROS-resistant phenotype that promotes metastasis. Nat Commun 10: 4862, 2019.
23. Infantino V, Santarsiero A, Convertini P, Todisco S and Iacobazzi V: Cancer cell metabolism in hypoxia: Role of HIF-1 as key regulator and therapeutic target. Int J Mol Sci 22: 5703, 2021.
24. Janbandhu V, Tallapragada V, Patrick R, Li Y, Abeygunawardena D, Humphreys DT, Martin EMMA, Ward AO, Contreras O, Farbehi N, *et al*: Hif-1a suppresses ROS-induced proliferation of cardiac fibroblasts following myocardial infarction. Cell Stem Cell 29: 281-297.e12, 2022.
25. Qin Y, Liu HJ, Li M, Zhai DH, Tang YH, Yang L, Qiao KL, Yang JH, Zhong WL, Zhang Q, *et al*: Salidroside improves the hypoxic tumor microenvironment and reverses the drug resistance of platinum drugs via HIF-1α signaling pathway. EBioMedicine 38: 25-36, 2018.
26. Sun L, Wu C, Ming J, Guo E, Zhang W, Li L and Hu G: EGLN1 induces tumorigenesis and radioresistance in nasopharyngeal carcinoma by promoting ubiquitination of p53 in a hydroxylase-dependent manner. J Cancer 13: 2061-2073, 2022.
27. Tang J, Deng H, Wang Z, Zha H, Liao Q, Zhu C, Chen X, Sun X, Jia S, Ouyang G, *et al*: EGLN1 prolyl hydroxylation of hypoxia-induced transcription factor HIF1α is repressed by SET7-catalyzed lysine methylation. J Biol Chem 298: 101961, 2022.
28. Zhou Y, Ouyang N, Liu L, Tian J, Huang X and Lu T: An EGLN1 mutation may regulate hypoxic response in cyanotic congenital heart disease through the PHD2/HIF-1A pathway. Genes Dis 6: 35-42, 2019.
29. Liu G, Zhao W, Zhang H, Wang T, Han Z and Ji X: rs1769793 variant reduces EGLN1 expression in skeletal muscle and hippocampus and contributes to high aerobic capacity in hypoxia. Proc Natl Acad Sci USA 117: 29283-29285, 2020.
30. Zhang G, Zhang D, Zhang X, Yu K and Jiang A: Saprirearine protects H9c2 cardiomyocytes against hypoxia/reoxygenation-induced apoptosis by activating Nrf2. Acta Biochim Pol 69: 429-436, 2022.
31 Su Y, Tian H, Wei L, Fu G and Sun T: Integrin β3 inhibits hypoxia-induced apoptosis in cardiomyocytes. Acta Biochim Biophys Sin (Shanghai) 50: 658-665, 2018.
32. Wang W, Li Q, Huang G, Lin BY, Lin D, Ma Y, Zhang Z, Chen T and Zhou J: Tandem mass tag-based proteomic analysis of potential biomarkers for hepatocellular carcinoma differentiation. Onco Targets Ther 14: 1007-1020, 2021.
33. Livak KJ and Schmittgen TD: Analysis of relative gene expression data using real-time quantitative PCR and the 2(-Delta Delta C(T)) method. Methods 25: 402-408, 2001.
34. Liang RP, Jia JJ, Li JH, He N, Zhou YF, Jiang L, Bai T, Xie HY, Zhou L and Sun YL: Mitofusin-2 mediated mitochondrial Ca^{2+} uptake 1/2 induced liver injury in rat remote ischemic perconditioning liver transplantation and alpha mouse liver-12 hypoxia cell line models. World J Gastroenterol 23: 6995-7008, 2017.
35. Salyha N and Oliynyk I: Hypoxia modeling techniques: A review. Heliyon 9: e13238, 2023.
36. Zhou W, Yang W, Fan K, Hua W and Gou S: A hypoxia-activated NO donor for the treatment of myocardial hypoxia injury. Chem Sci 13: 3549-3555, 2022.
37. Wen SY, Tamilselvi S, Shen CY, Day CH, Chun LC, Cheng LY, Ou HC, Chen RJ, Viswanadha VP, Kuo WW and Huang CY: Protective effect of HDL on NADPH oxidase-derived super oxide anion mediates hypoxia-induced cardiomyocyte apoptosis. PLoS One 12: e0179492, 2017.
38. Sun S, Tuo Q, Li D, Wang X, Li X, Zhang Y, Zhao G and Lin F: Antioxidant effects of salidroside in the cardiovascular system. Evid Based Complement Alternat Med 2020: 9568647, 2020.
39. Ni J, Li Y, Xu Y and Guo R: Salidroside protects against cardiomyocyte apoptosis and ventricular remodeling by AKT/HO-1 signaling pathways in a diabetic cardiomyopathy mouse model. Phytomedicine 82: 153406, 2021.
40. Li M, Li K and Ren Y: Nesfatin-1 protects H9c2 cardiomyocytes against cobalt chloride-induced hypoxic injury by modulating the MAPK and Notch1 signaling pathways. J Biol Res (Thessalon) 28: 21, 2021.
41. Lee HR, Leslie F and Azarin SM: A facile in vitro platform to study cancer cell dormancy under hypoxic microenvironments using $CoCl_2$. J Biol Eng 12: 12, 2018.
42. Xu Z, Zhang D, He X, Huang Y and Shao H: Transport of calcium ions into mitochondria. Curr Genomics 17: 215-219, 2016.
43. Zhang Y, Li L, Yue J, Cao L, Liu P, Dong WF and Liu G: Yttrium-mediated red fluorescent carbon dots for sensitive and selective detection of calcium ions. Luminescence 36: 1969-1976, 2021.

44. Bao W, Liu M, Meng J, Liu S, Wang S, Jia R, Wang Y, Ma G, Wei W and Tian Z: MOFs-based nanoagent enables dual mitochondrial damage in synergistic antitumor therapy via oxidative stress and calcium overload. Nat Commun 12: 6399, 2021.
45. Zheng P, Ding B, Jiang Z, Xu W, Li G, Ding J and Chen X: Ultrasound-augmented mitochondrial calcium ion overload by calcium nanomodulator to induce immunogenic cell death. Nano Lett 21: 2088-2093, 2021.
46. Zhou Q, Xie M, Zhu J, Yi Q, Tan B, Li Y, Ye L, Zhang X, Zhang Y, Tian J and Xu H: PINK1 contained in huMSC-derived exosomes prevents cardiomyocyte mitochondrial calcium overload in sepsis via recovery of mitochondrial Ca^{2+} efflux. Stem Cell Res Ther 12: 269, 2021.
47. Chen SF, Pan MX, Tang JC, Cheng J, Zhao D, Zhang Y, Liao HB, Liu R, Zhuang Y, Zhang ZF, *et al*: Arginine is neuroprotective through suppressing HIF-1α/LDHA-mediated inflammatory response after cerebral ischemia/reperfusion injury. Mol Brain 13: 63, 2020.
48. Kim JW, Tchernyshyov I, Semenza GL and Dang CV: HIF-1-mediated expression of pyruvate dehydrogenase kinase: A metabolic switch required for cellular adaptation to hypoxia. Cell Metab 3: 177-185, 2006.
49. Wu D, Wang S, Wang F, Zhang Q, Zhang Z and Li X: Lactate dehydrogenase A (LDHA)-mediated lactate generation promotes pulmonary vascular remodeling in pulmonary hypertension. J Transl Med 22: 738, 2024.
50. Meng F, Zhang W and Wang Y: RASAL1 inhibits HepG2 cell growth via HIF-2α mediated gluconeogenesis. Oncol Lett 14: 7344-7352, 2017.
51. Wu X and Chen S: Advances in natural small molecules on pretranslational regulation of gluconeogenesis. Drug Dev Res 84: 613-628, 2023.